

Changes in Nanoscale Chain Assembly in Sweet Potato Starch Lamellae by Downregulation of Biosynthesis Enzymes

Binjia Zhang, Wenzhi Zhou, Dongling Qiao, Zhang Peng, Si-ming Zhao, Liang Zhang, and Fengwei Xie

J. Agric. Food Chem., **Just Accepted Manuscript** • DOI: 10.1021/acs.jafc.8b06523 • Publication Date (Web): 29 Mar 2019

Downloaded from <http://pubs.acs.org> on March 30, 2019

Just Accepted

“Just Accepted” manuscripts have been peer-reviewed and accepted for publication. They are posted online prior to technical editing, formatting for publication and author proofing. The American Chemical Society provides “Just Accepted” as a service to the research community to expedite the dissemination of scientific material as soon as possible after acceptance. “Just Accepted” manuscripts appear in full in PDF format accompanied by an HTML abstract. “Just Accepted” manuscripts have been fully peer reviewed, but should not be considered the official version of record. They are citable by the Digital Object Identifier (DOI®). “Just Accepted” is an optional service offered to authors. Therefore, the “Just Accepted” Web site may not include all articles that will be published in the journal. After a manuscript is technically edited and formatted, it will be removed from the “Just Accepted” Web site and published as an ASAP article. Note that technical editing may introduce minor changes to the manuscript text and/or graphics which could affect content, and all legal disclaimers and ethical guidelines that apply to the journal pertain. ACS cannot be held responsible for errors or consequences arising from the use of information contained in these “Just Accepted” manuscripts.



1 Changes in Nanoscale Chain Assembly in Sweet
2 Potato Starch Lamellae by Downregulation of
3 Biosynthesis Enzymes

4 Binjia Zhang^a, Wenzhi Zhou^b, Dongling Qiao^c, Peng Zhang^{*b}, Siming Zhao^a, Liang Zhang^d,
5 Fengwei Xie^{†,e,f}

6 ^a Group for Cereals and Oils Processing, Key Laboratory of Environment Correlative Dietology (Ministry of
7 Education), College of Food Science and Technology, Huazhong Agricultural University, Wuhan 430070, China

8 ^b National Key Laboratory of Plant Molecular Genetics, CAS Center for Excellence in Molecular Plant Sciences,
9 Institute of Plant Physiology and Ecology, Shanghai Institutes for Biological Sciences, Chinese Academy of
10 Sciences, Shanghai 200032, China

11 ^c Glyn O. Phillips Hydrocolloid Research Centre at HBUT, Hubei University of Technology, Wuhan 430068, China

12 ^d School of Food Science and Engineering, Yangzhou University, Yangzhou 225127, China

13 ^e Institute of Advanced Study, University of Warwick, Coventry CV4 7HS, United Kingdom

14 ^f International Institute for Nanocomposites Manufacturing (IINM), WMG, University of Warwick, Coventry CV4
15 7AL, United Kingdom

16

17 **KEYWORDS:** Starch; Semicrystalline lamellae; Molecular chain features; X-ray scattering

18 **ABSTRACT:** Granule-bound starch synthase I (GBSSI) and starch branching enzyme I and II
19 (SBEI and SBEII) are crucial enzymes biosynthesizing starches with varied apparent amylose

20 content and amylopectin branching structure. With a sweet potato (*Ipomoea batatas* [L.] Lam.)
21 Cv. Xushu22, this work shows that downregulating GBSSI (for waxy starch) or SBE (for high-
22 amylose starch) activity allowed the formation of new semicrystalline lamellae (named Type II)
23 in sweet potato starch in addition to the widely reported Type I lamellae. Small-angle X-ray
24 scattering (SAXS) results show that, compared to Type I lamellae, Type II lamellae displayed
25 increased average thickness and thickness distribution width, with thickened amorphous and
26 crystalline components. The size-exclusion chromatography (SEC) data revealed mainly two
27 enzyme-sets (i and ii) synthesizing amylopectin chains. Reducing the GBSSI or SBE activity
28 increased the amounts of amylopectin long chains (degree of polymerization (DP) ≥ 33).
29 Combined SAXS and SEC analyses indicate that part of these long chains from enzyme-set (i)
30 could be confined to Type II lamellae, followed by $DP \leq 32$ short chains in Type I lamellae and
31 the rest long chains from enzyme-sets (i) and (ii) spanning more than a single lamella.

32

33 **Introduction**

34 In green plants, the biosynthesis of natural polymers, such as starch, protein and cellulose, stands
35 at the core of providing agro-resources for food and non-food products with demanded features.
36 Starch, a storage carbohydrate in plants (*e.g.*, maize, wheat, rice, potato, cassava, sweet potato),
37 normally serves as a crucial food ingredient offering energy for humans. The biosynthesis of starch
38 is mainly governed by four categories of enzymes, namely, ADP-glucose pyrophosphorylase
39 (AGPase), starch synthases (SSs), starch branching enzymes (SBEs) and starch debranching
40 enzymes (DBEs).¹⁻² Modulating the activities of starch biosynthetic enzymes could be a cost-
41 effective approach for the production of starch resources with tailored structure and properties.

42 Two major starch polymers are biosynthesized during plant growth, namely, relatively linear
43 amylose and highly branched amylopectin.³ The molecular chains of amylose and amylopectin can
44 assemble on different length scales to form a multilevel structural system of the starch granule,
45 including the whole granule, growth rings, blocklets, semicrystalline lamellae, crystalline
46 structure, and double/single helices.³⁻⁶ The multi-level structural features are closely related to
47 starch properties. To date, maize, rice, and sweet potato starches with varied apparent amylose
48 content (0% to > 50%) and amylopectin branching structure have been produced through
49 modifying the activities of biosynthetic enzymes such as granule-bound starch synthase (GBSS),
50 and/or SBE.⁷⁻⁸ Compared to the wild-type (WT) starch and the waxy starch with GBSS
51 downregulation, the high-amylose starches (apparent amylose content > 50%) with SBE
52 downregulation show an enhanced granule surface density but a reduced crystallinity degree with
53 B-type crystallites and eventually unique properties such as reduced enzyme susceptibility,⁹⁻¹⁰
54 higher gelatinization temperature,¹¹ and altered rheological features.¹² Consequently, the high-
55 amylose starches have versatile potentials for functional foods with low glycemic indexes and for

56 high-performance materials with fascinating functions (*e.g.*, bioactive compound delivery).
57 However, though the main assembly of starch chains on the nanoscale is the semicrystalline
58 lamellar structure, it is still not fully understood how the amylose-content-related biosynthetic
59 enzymes (*e.g.*, GBSS and SBE) tailor the features of starch lamellae, which subsequently
60 determine the starch properties and functionality.

61 The starch lamellae can be characterized using small-angle X-ray scattering (SAXS) technique
62 with the paracrystalline model,¹³⁻¹⁴ the liquid-crystalline model¹⁵ and the linear correlation
63 function.¹⁶ A series of lamellar parameters such as the average thickness of semicrystalline
64 lamellae can be obtained for starches from various origins, *e.g.*, wheat, maize, rice, potato, cassava,
65 and water chestnut.¹⁷⁻²¹ It is noteworthy that the change in apparent amylose content probably
66 alters starch lamellar features.^{9, 19} For instance, compared to regular starch, high-amylose starches
67 from potato display different lamellar packing whose features can be evaluated using the scattering
68 data and the paracrystalline model with a stacking disorder nature.¹⁹ Nonetheless, to model the
69 structural parameters, this study still needs complicated predefined assumptions for the lamellar
70 structure and the usage of fixed values for partial parameters. Thus, it remains challenging to
71 simply and straightforwardly calculate the lamellar parameters of starches with varied apparent
72 amylose content and amylopectin branching structure from the SAXS data. In addition, starch
73 chains can assemble into crystalline lamellae to construct semicrystalline growth rings.
74 Consistently, the chain length distributions (CLDs) are capable of affecting the lamellar parameters
75 of rice starches with apparent amylose content up to 24%.²²⁻²³ However, the previous studies did
76 not concern how the biosynthetic enzymes (*e.g.*, GBSS and SBE) alter the CLDs of starch and thus
77 its nanoscale chain assembly in lamellae, with apparent amylose content in much wider ranges
78 such as from 0% to >50%.

79 To this end, a WT sweet potato (*Ipomoea batatas* [L.] Lam.) and its waxy (produced by granule-
80 bound starch synthase I (GBSSI) with downregulated activity) and high-amylose (produced by
81 SBE with downregulated activity) lines were used as the model plants for the biosynthesis of WT
82 and tailored starches with *ca.* 6% to 65% apparent amylose content. The small angle X-ray
83 scattering (SAXS) technique was applied to characterize the semicrystalline lamellae of the
84 starches. Interestingly, a new type of semicrystalline lamellae was found and a fitting method was
85 proposed to resolve the lamellar peak and its subpeaks from the whole SAXS pattern. The fitted
86 lamellar peaks were used to straightforwardly calculate the fine parameters for the two types of
87 starch lamellae with a linear correlation function. Along with that, the CLDs of starch and the
88 related starch biosynthetic enzyme activities were analyzed using the SEC data. Then, from a CLD
89 point of view, we discussed how the GBSSI or SBE downregulation tailors the starch lamellar
90 structure.

91 **Experimental Section**

92 **Materials.** The sweet potato (*Ipomoea batatas* [L.] Lam.) Cv. Xushu22, a widely used cultivar
93 for starch production in China, was used as the donor cultivar (WT) for modification. A method
94 described previously²⁴ was applied to generate modified sweet potato plants. One waxy line
95 (namely Waxy-91) with downregulated GBSSI expression and three high-amylose lines (HAM-
96 75, HAM-214, and HAM-234) with downregulated SBE expression were chosen for this study.
97 The expressions of SBEI (GenBank Accession No. AB071286.1) and SBEII (GenBank Accession
98 No. AB194723.1) were downregulated. The WT plant and its modified lines were cultivated in the
99 experimental station, Demonstration Base for Molecular Breeding and New Variety of Sweet
100 Potato (117°15'16", 36°5'56") in Tai'an City (Shandong, China) in early May 2014. The storage
101 roots were harvested in the mid of October 2014, and the starches were isolated using an earlier

102 method.²⁵ The obtained starches were dried in an oven at 40 °C for 1 day and were ground and
103 stored in a low-humidity cabinet HZD-1000 (Biofuture Ltd., Beijing, China) for further analyses.
104 As measured using an iodine colorimetric method^{7,26}, the apparent amylose content for WT and
105 Waxy-91 was (30.4±0.6)% and (6.7±1.0)%, respectively, while HAM-75, HAM-214, and HAM-
106 234 had apparent amylose contents of (50.3±2.5)%, (65.5±0.6)%, and (61.0±2.6)%, respectively
107 (shown in **Table 1**). The WT and waxy sweet potato starches showed an A-type crystalline
108 structure, and the high-amylose ones presented B-type structures (see XRD patterns in **Fig. S1** in
109 **Supplementary Material**).

110 **Small-angle X-ray Scattering (SAXS).** SAXS measurements were conducted on a NanoSTAR
111 system (Bruker, Germany) operated at 30 W. The Cu K α radiation²⁷ having a 0.1542 nm
112 wavelength (λ) was used as the X-ray source. Before the SAXS tests, the starch slurries with a
113 starch concentration of *ca.* 40% were kept under ambient conditions for 4 h to achieve equilibrium
114 samples. According to previous research,²⁸⁻²⁹ dry starch is in the glassy nematic state, whereas the
115 hydrated starch forms a lamellar smectic structure with highly mobile backbone and spacers. Each
116 starch slurry was placed into the sample cell, which was then exposed at the incident X-ray
117 monochromatic beam for 15 min. The scattering data were collected using a VÅnTeC-2000
118 detector (active area 140 × 140 mm² and pixel size 68 × 68 μ m²). The scattering of an empty cell
119 with water was used as the background data. All data were background subtracted and normalized.
120 The data in the region of *ca.* 0.007 < q < 0.20 Å⁻¹ were used as the SAXS results. The scattering
121 vector, q (Å⁻¹), was defined as $q = 4\pi\sin\theta/\lambda$ (2θ , the scattering angle).³⁰

122 **Fitting and Analysis of SAXS data.** A fitting approach with two Gaussian plus Lorentz peak
123 functions and a power-law function was established to fit the SAXS patterns. The SAXS data were
124 fitted iteratively in Origin 8 software (OriginLab. Inc., USA). The fitting coefficients for each

125 iteration were refined to minimize the value of chi-squared via a nonlinear, least-squares
126 refinement method. Then, the structural features of starch semicrystalline lamellae were calculated
127 using the linear correlation function (presented in **Eq.(5)**).³¹⁻³³

128 **Size-exclusion Chromatography (SEC).** The SEC experiments were conducted according to
129 an earlier method with modifications.³⁴ The starch was dissolved in a DMSO/LiBr solution
130 containing 0.5% (w/w) LiBr. The possibly-existing non-starch polysaccharides such as cellulose
131 in the sample are mostly insoluble, and were removed by centrifuging the starch-DMSO solution
132 at 4000 g for 10 min. The supernatant was mixed with ethanol (6 volumes of DMSO/LiBr) to
133 precipitate the starch, and the precipitated starch was collected by centrifugation at 4000 g for
134 10 min. The precipitated starch was dissolved in DMSO/LiBr at 80 °C overnight. The starch
135 concentration in DMSO/LiBr was determined using the Megazyme total starch assay kit and
136 adjusted to 2 mg/mL for SEC analysis. Briefly, the starch solution was centrifuged at 4000 g for
137 10 min; 2 mL of the supernatant was digested and the glucose released from starch was determined
138 by absorbance at a wavelength of 510 nm using the procedures given by the assay kit manufacturer.
139 To obtain the chain length distributions (CLDs) of debranched starch molecules, the starch samples
140 were debranched using isoamylase according to a previous method.³⁵ The Agilent 1100 Series
141 SEC system was used, with GRAM precolumn, GRAM 100 and GRAM 1000 columns (PSS,
142 Germany) at a flow rate of 0.6 mL/min. For the debranched starch containing linear molecules, the
143 value of hydrodynamic volume V_h was converted to the degree of polymerization (DP) using the
144 Mark–Houwink equation.³⁶

145 **Starch Biosynthetic Enzyme Activities Fitted from Number CLDs.** A mathematical model
146 was used to fit the number CLDs of debranched amylopectin to parameterize the relative activities
147 of three core classes of starch biosynthetic enzymes, namely, SSs including GBSS, SBE and

148 DBE.³⁷⁻³⁸ A theoretical “enzyme set” is defined as a groups of these three enzymes, which includes
149 one of SS, SBE, and DBE, regardless of the actual informs.³⁷⁻³⁸ In the present work, the
150 amylopectin CLDs were mainly contributed by enzyme-sets (i) and (ii).

151 **Statistical Analysis.** Data were expressed as means \pm standard deviations (SD) and were
152 statistically analyzed using IBM SPSS software version 20.0 (Chicago, IL, USA). A statistical
153 difference of $P < 0.05$ was considered to be significant.

154 **Results and Discussion**

155 **General Features of SAXS Data.** The logarithmic SAXS patterns of WT and modified sweet
156 potato starches are presented in **Fig. S2**. The starches displayed a typical scattering peak at *ca.*
157 0.065 \AA^{-1} (labelled as Peak I), ascribed to the widely-reported semicrystalline lamellae in starch.³⁹
158 Interestingly, the high-amylose starches, resulting from the downregulated SBE activity, had a less
159 resolved shoulder peak at *ca.* 0.040 \AA^{-1} (labelled as Peak II). Such dual-peak scattering pattern of
160 starch semicrystalline lamellae was different from the extensively found results where a single
161 lamellar peak was shown^{33, 39}. The results here confirmed the existence of a notable proportion of
162 thicker semicrystalline lamellae (proposed as Type II shown by Peak II) in the high-amylose
163 starches, other than the typical Type I semicrystalline lamellae revealed by the Peak I at *ca.*
164 0.065 \AA^{-1} .

165 Research has shown the SAXS data of high-amylose maize starches, which have a typical single
166 lamellar peak.^{10, 40} Also, the SAXS data for high-amylose potato starches at q values higher than
167 0.02 \AA^{-1} were collected.¹⁹ It seems that the used q range could not sufficiently cover the lamellar
168 peak especially at the low angles, and thus it is difficult to observe the full information of lamellar
169 scattering possibly including a dual-peak pattern. In that case, the paracrystalline model
170 accompanied by stacking disorder was applied to describe the lamellar structure, followed by

171 complicated predefined assumptions of the lamellar stacking and the usage of partial constant
 172 lamellar parameters before data fitting.¹⁹ Here, the scattering data in the range of *ca.* $0.007 < q <$
 173 0.20 \AA^{-1} were recorded for the sweet potato starches to show the full dual-peak pattern associated
 174 with the lamellar structure of the amylose-rich starches. In the following, a fitting method based
 175 on combined functions (*e.g.*, Gaussian, Lorentz, and power law) was established to fit the net
 176 lamellar scattering from the SAXS data. Then, the fitted lamellar scattering was used to acquire
 177 the linear correlation function profile with the elimination of non-lamellar scattering.⁴¹ In this way,
 178 the fine parameters of the two sub-lamellar fractions (Type I and Type II) with increased accuracy
 179 could be calculated straightforwardly.

180 **Fitting of SAXS Data.** Two Gaussian plus Lorentz peak functions and a power-law function
 181 (Eq. (1)-(3)) were used to fit the scattering data for the high-amylose sweet potato starches with
 182 unresolved Peak I and Peak II. This dual-peak fitting method was also applied for the waxy starch
 183 (with downregulated GBSSI activity) that did not show a prominent Peak II (**Fig. S2** in
 184 **Supplementary Material**), since using only one Gaussian plus Lorentz peak function could not
 185 sufficiently fit the scattering pattern (see the single-peak fitting for waxy starch in **Fig. S3** in
 186 **Supplementary Material**). Nevertheless, for the WT starch, one Gaussian plus Lorentz peak
 187 function (with a power-law function) was enough for the desired fitting.

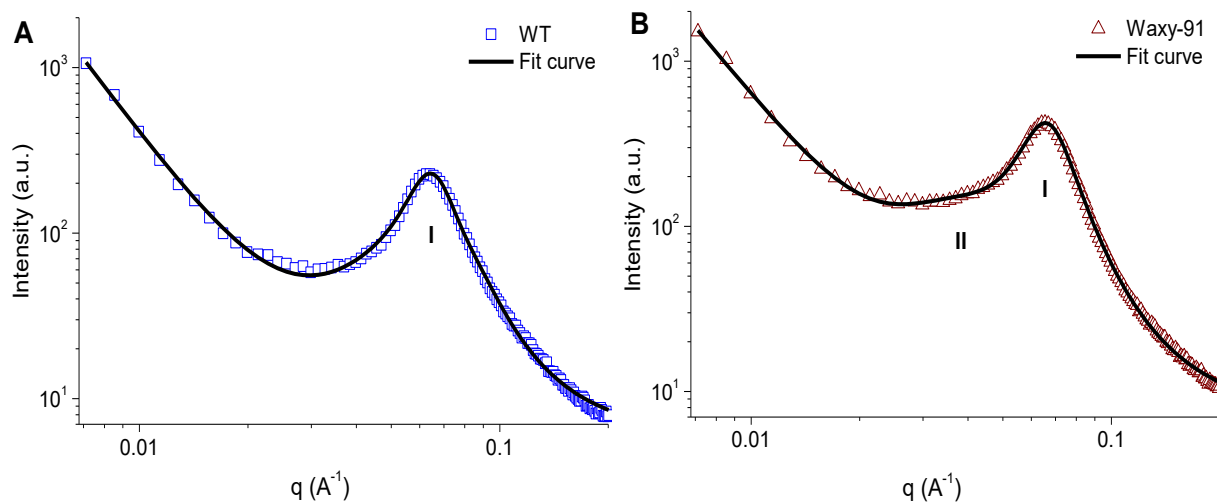
$$188 \quad I(q) = B + C * q^{-\delta} + f_1 * G_1(q) + (1 - f_1) * L_1(q) + f_2 * G_2(q) + (1 - f_2) * L_2(q) \quad (1)$$

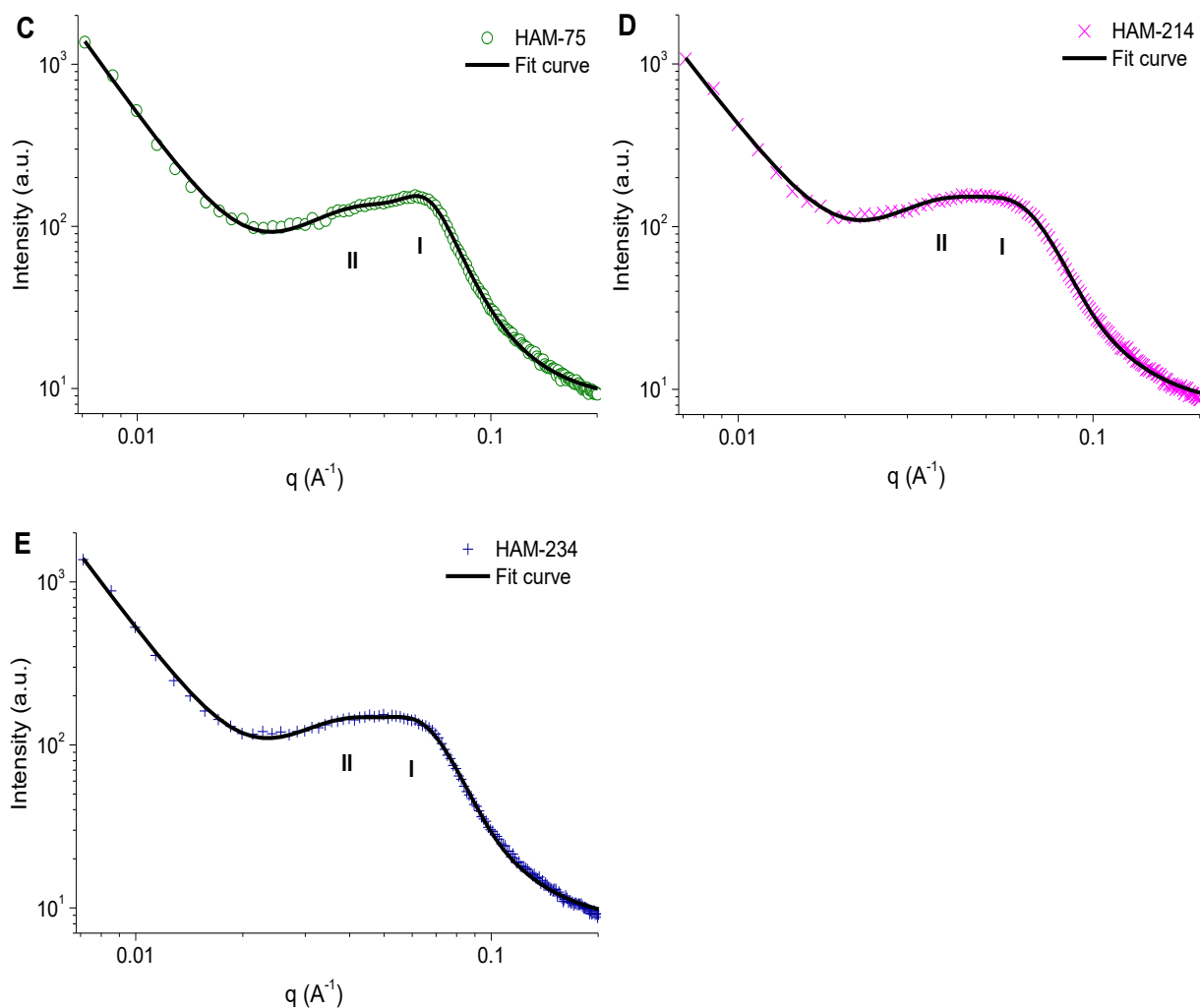
$$189 \quad G_x(q) = \frac{A_x \sqrt{\ln 4}}{W_x \sqrt{\frac{\pi}{2}}} \exp\left(-\frac{2 \ln 4 (q - q_x)^2}{W_x^2}\right) \quad (2)$$

$$190 \quad L_x(q) = \frac{2A_x}{\pi} * \frac{2W_x}{4(q - q_x)^2 + W_x^2} \quad (3)$$

191 In Eq. (1), the first term, B , is the scattering background; the second term, the power-law function
192 in which C and δ are the power-law prefactor and the power-law component, respectively; the
193 third or fifth term, the Gaussian function; the fourth or sixth term, the Lorentz function; f_1 and f_2 ,
194 the prefactors for Peak I at *ca.* 0.065 \AA^{-1} and Peak II at *ca.* 0.040 \AA^{-1} , respectively. Again, in Eq.
195 (2) (Gaussian function, $G_x(q)$) and Eq. (3) (Lorentz function, $L_x(q)$), A_x is the peak area, W_x (\AA^{-1})
196 the peak full width at half-maximum (*FWHM*) in reciprocal space, and q_x (\AA^{-1}) the peak center
197 position; $x = 1$ and $x = 2$ correspond to Peak I and Peak II, respectively. **Fig. 1** shows the SAXS
198 patterns and their fit curves for WT and modified sweet potato starches. The results show that all
199 SAXS patterns could be properly fitted using the above established fitting approach with Eqs. (1)-
200 (3).

201





203

204

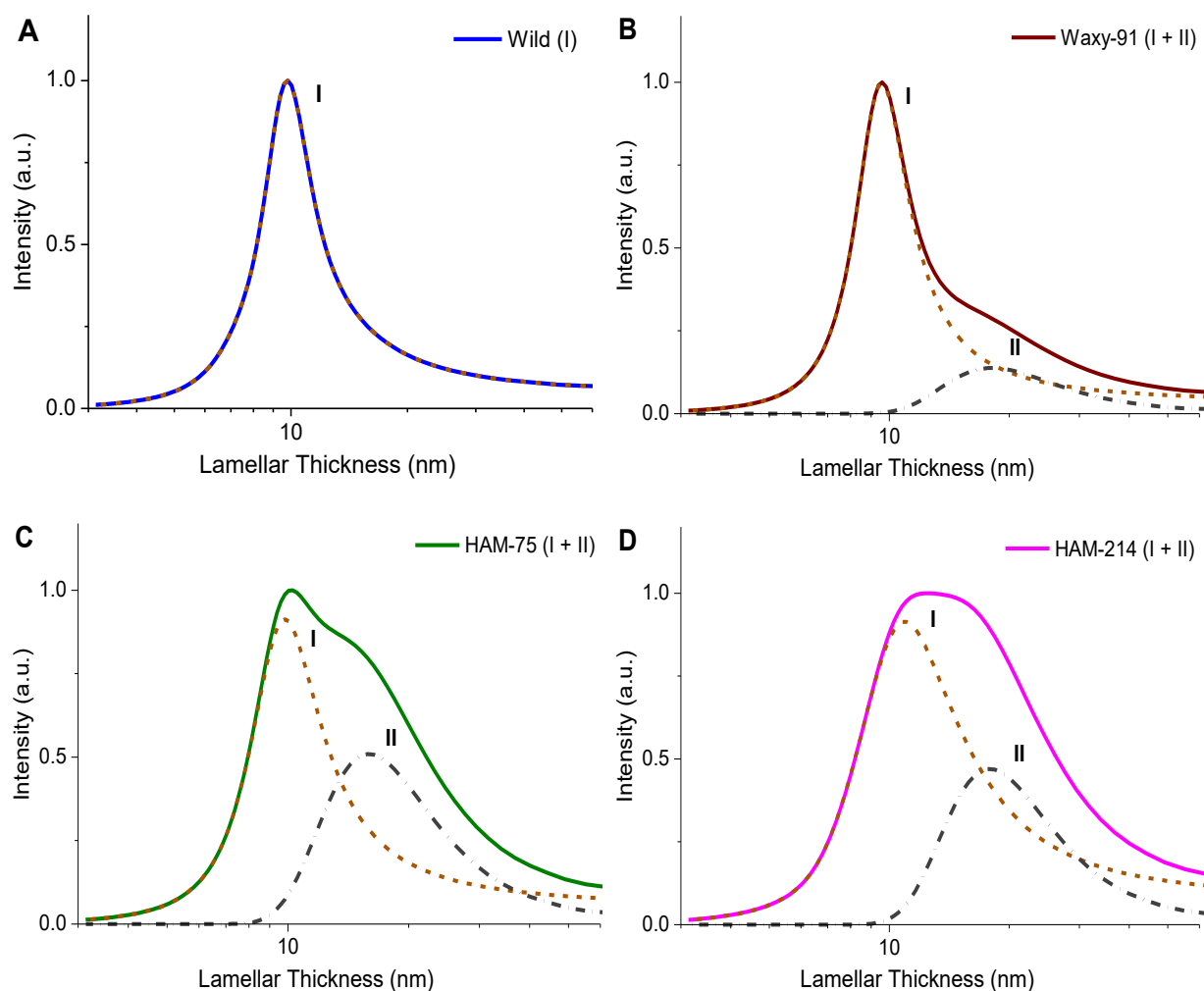
205 **Fig. 1** Logarithmic SAXS patterns and their fit curves of wild-type (WT) (A) and modified (Waxy-
 206 91, HAM-75, HAM-214 and HAM-234) (B-E) sweet potato starches.

207

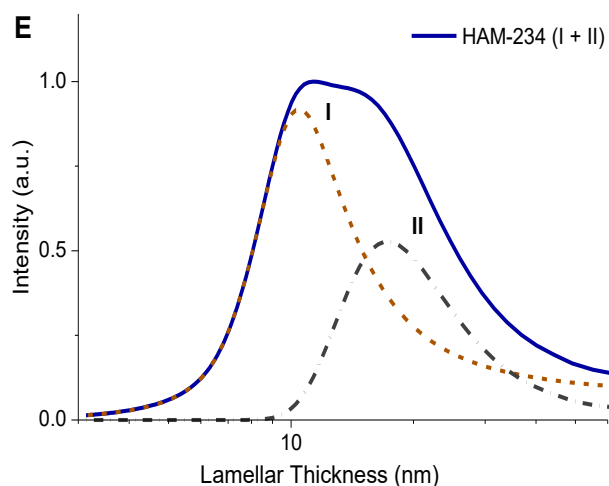
208 **Thickness Distribution of Semicrystalline Lamellae.** By subtracting the background
 209 scattering (1st term in Eq. (1)) and the power-law scattering (2nd term in Eq. (1)) from the whole
 210 SAXS pattern, the net scattering of lamellar peak could be acquired. Then, the ordinate scattering
 211 intensity was normalized using its maximum, and the abscissa q values were transformed into
 212 lamellar thickness values equal to $2\pi/q$. Consequently, the thickness distribution profiles of
 213 semicrystalline lamellae were revealed for sweet potato starches (**Fig. 2**). The WT starch contained

214 only Type I semicrystalline lamellae with a single-peak thickness distribution mainly in the range
215 of predominantly 5–20 nm. Nonetheless, the waxy and high-amylose starches displayed a dual-
216 peak lamellar thickness distribution, as they had additional Type II semicrystalline lamellae with
217 a thickness distribution range of mainly 10–50 nm. Note that the waxy sample showed a very weak
218 Type II distribution. That is, compared to GBSSI downregulation, the downregulated SBE activity
219 more effectively induced the formation of Type II semicrystalline lamellae in addition to typical
220 Type I lamellae. This is associated with the altered arrangement of biosynthesized starch molecule
221 chains within the lamellar regions, as discussed especially in the last section.

222



224



225
 226 **Fig. 2** Semicrystalline lamellar thickness distributions of wild-type (WT) (A) and modified (Waxy-
 227 91, HAM-75, HAM-214 and HAM-234) (B-E) sweet potato starches. Solid lines represent whole
 228 distribution profiles; short dash lines represent profiles related to Type I semicrystalline lamellae;
 229 dash-dot lines represent profiles related to Type II semicrystalline lamellae.

230
 231 **Table 1** shows the fitted peak positions (q_1 and q_2) and $FWHM$ values in reciprocal space (W_1
 232 and W_2) for the subpeaks I and II. Then, $FWHM$ in reciprocal space was converted into the real
 233 space value with Eq. (4). This real space value is positive to the thickness distribution width of
 234 semicrystalline lamellae.⁴²

$$235 \quad FWHM(\text{real}) = \frac{2\pi W_x}{q_x^2} \quad (4)$$

236 Here, W_x (\AA^{-1}) is the $FWHM$ in reciprocal space, and q_x (\AA^{-1}) the peak position; subscript $x = 1$
 237 and $x = 2$ belong to Peak I and Peak II, respectively. In **Table 1**, Type II lamellae had a larger
 238 $FWHM$ value than did Type I lamellae. Enhancing SBE downregulation (shown by increased
 239 apparent amylose content) led to a gradual increase in $FWHM$ for Type I lamellae of all the
 240 starches, and a modest increase in this parameter for Type II lamellae of the high-amylose samples.

241 Relative to the amylose-rich starches, the waxy starch had a slightly-increased *FWHM* of Type II
242 lamellae.

243

244 **Table 1** Apparent amylose content and SAXS parameters of wild-type (WT) and modified (Waxy-
245 91, HAM-75, HAM-214 and HAM-234) sweet potato starches ^A

	WT	Waxy-91	HAM-75	HAM-214	HAM-234
<i>AC</i>	30.4±0.6 ^d	6.7±1.0 ^e	50.3±2.5 ^c	65.5±0.6 ^a	61.0±2.6 ^b
δ	2.92±0.02 ^{bc}	2.67±0.03 ^d	3.09±0.03 ^a	2.88±0.03 ^c	2.96±0.03 ^b
Peak I <i>A</i> ₁	4.05±0.12 ^b	8.33±0.14 ^a	3.43±0.50 ^c	4.58±1.11 ^{bc}	4.15±0.88 ^{bc}
<i>q</i> ₁ (Å ⁻¹)	0.0642±0.0001 ^b	0.0656±0.0002 ^a	0.0640±0.0013 ^{bc}	0.0575±0.0036 ^d	0.0600±0.0028 ^{cd}
<i>W</i> ₁ (Å ⁻¹)	0.0256±0.0005 ^c	0.0259±0.0004 ^c	0.0330±0.0019 ^b	0.0417±0.0042 ^a	0.0391±0.0036 ^a
<i>FWHM</i> ₁ (nm)	3.90±0.07 ^d	3.77±0.05 ^e	5.05±0.08 ^c	7.92±0.19 ^a	6.82±0.03 ^b
Peak II <i>A</i> ₂	-	1.59±0.18 ^b	2.29±0.46 ^a	1.80±0.96 ^{ab}	2.04±0.77 ^{ab}
<i>q</i> ₂ (Å ⁻¹)	-	0.0347±0.0009 ^b	0.0395±0.0018 ^a	0.0352±0.0023 ^b	0.0364±0.0022 ^{ab}
<i>W</i> ₂ (Å ⁻¹)	-	0.0263±0.0027 ^a	0.0294±0.0034 ^a	0.0255±0.0049 ^a	0.0265±0.0042 ^a
<i>FWHM</i> ₂ (nm)	-	13.70±0.74 ^a	11.79±0.30 ^b	12.92±0.86 ^{ab}	12.52±0.50 ^{ab}
<i>Chi</i> ²	26.68	58.39	39.81	32.78	42.81

246 ^A *AC*, apparent amylose content (%). Parameters from SAXS data fitting: δ , power-law exponent;
247 *A*₁ or *A*₂, lamellar peak area; *q*₁ or *q*₂, lamellar peak position; *W*₁ or *W*₂, peak full width at half
248 maximum in reciprocal space; *FWHM*₁ or *FWHM*₂, peak full width at half maximum in real space;
249 *Chi*², reduced Chi-square of fitting.

250 ^B The different inline letters within a row indicate significant difference *P* < 0.05.

251

252 **Average Thicknesses of Semicrystalline, Amorphous and Crystalline Lamellae.** The fitted
253 net lamellar peak and its two subpeaks from the whole SAXS pattern were used to calculate the

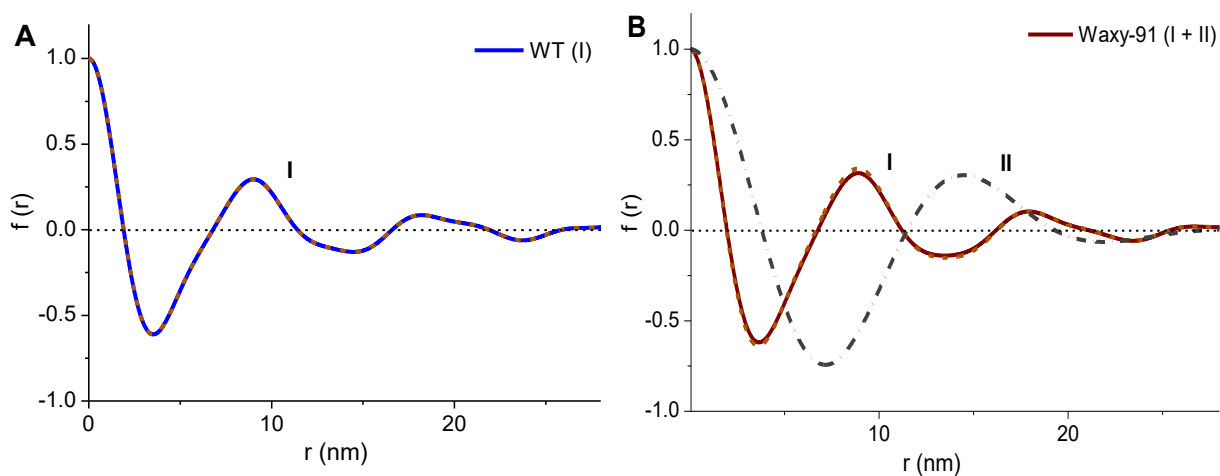
254 parameters of starch semicrystalline lamellae with increased accuracy.⁴¹ This was achieved using
 255 the linear correlation function $f(r)$ in Eq. (5) and **Fig. S4** in **Supplementary Material**.³¹⁻³²

$$256 \quad f(r) = \frac{\int_0^{\infty} I(q)q^2 \cos(qr) dq}{\int_0^{\infty} I(q)q^2 dq} \quad (5)$$

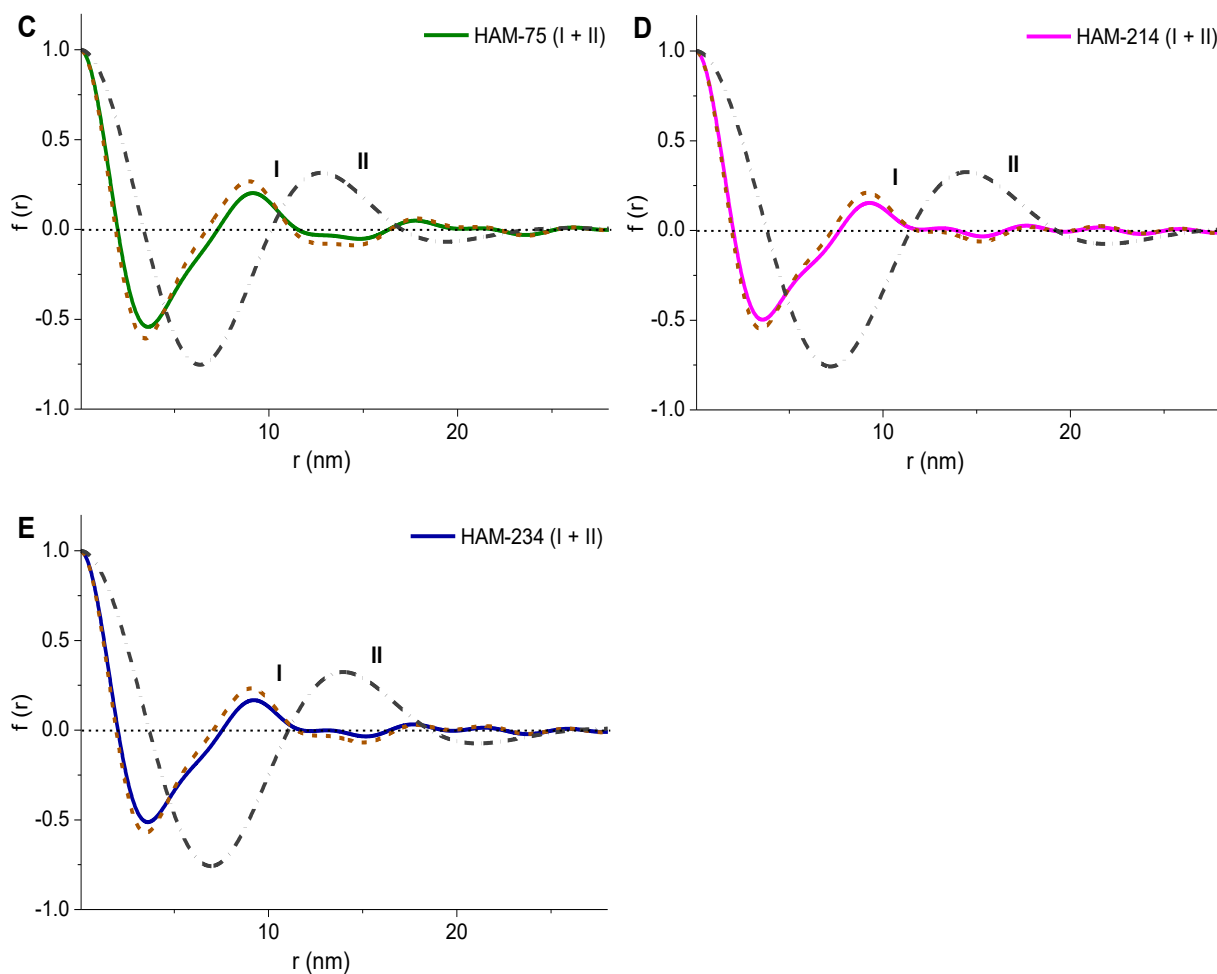
257 In Eq. (5), r (nm) is the distance in real space. In **Fig. S4** in **Supplementary Material**, d is the
 258 second maximum of $f(r)$ (equal to the average thickness of semicrystalline lamellae); d_a , the
 259 average thickness of amorphous lamellae, is acquired by the solution of the linear region and the
 260 flat $f(r)$ minimum; d_c , the average thickness of crystalline lamellae, is calculated by $d_c = d - d_a$.

261 **Fig. 3** includes the whole linear correlation function profiles and their subprofiles related to Type
 262 I or Type II semicrystalline lamellae for WT and modified sweet potato starches. The second
 263 maximum abscissa value (d) of the Type II profile (dash-dot line) was larger than that of the Type
 264 I profile (short dash line). Consequently, this abscissa value of the whole profile (real line), related
 265 to both Type I and Type II lamellae, ranged somewhere between those two values for the Type I
 266 profile and the Type II profile, respectively. Also, relative to the high-amylose starches, the waxy
 267 starch had a small Peak II, and thus showed a whole profile close to the Type I profile (**Fig. 3B**).

268



269



270

271

272 **Fig. 3** Linear correlation function profiles of wild-type (WT) (A) and modified (Waxy-91, HAM-
 273 75, HAM-214 and HAM-234) (B-E) sweet potato starches. The solid line represents the whole
 274 profile; the short dash line represents the profile related to Type I semicrystalline lamellae; the
 275 dash-dot line represents the profile related to Type II semicrystalline lamellae.

276

277 **Table 2** records the lamellar parameters for WT and modified sweet potato starches. Relative to
 278 Type I lamellae, Type II lamellae showed thicker amorphous (d_a) and crystalline (d_c) parts, and
 279 thus an elevated average thickness (d). For Type I lamellae in high-amylose starches, d_c showed
 280 the same trend as d with negligibly changed d_a . This suggests that the downregulated SBE activity

281 could increase the average thickness of Type I lamellae by thickening the crystalline components
 282 rather than the amorphous lamellae. However, Type I lamellae in the waxy sample (with reduced
 283 GBSSI expression) had a slight decrease in d_c and an increase in d_a , showing a slightly reduced d
 284 relative to that for the WT starch. For Type II lamellae, d_c and d_a showed a constant trend to d ,
 285 suggesting that the reduced GBSSI or SBE activity tended to simultaneously change the average
 286 thicknesses of amorphous and crystalline components with aligned starch molecule chains and
 287 thus the overall average thickness.

288

289 **Table 2** Lamellar parameters of wild-type (WT) and modified (Waxy-91, HAM-75, HAM-214
 290 and HAM-234) sweet potato starches ^A

	WT	Waxy-91	HAM-75	HAM-214	HAM-234
Lamellae I d_1 (nm)	9.01±0.03 ^{CB}	8.89±0.04 ^d	8.93±0.03 ^d	9.17±0.04 ^a	9.08±0.03 ^b
d_{c-1} (nm)	6.27±0.02 ^c	6.08±0.02 ^e	6.23±0.00 ^d	6.47±0.01 ^a	6.37±0.01 ^b
d_{a-1} (nm)	2.74±0.01 ^b	2.81±0.02 ^a	2.70±0.03 ^b	2.70±0.03 ^b	2.71±0.02 ^b
Lamellae II d_2 (nm)	-	14.47±0.06 ^a	12.78±0.04 ^c	14.48±0.07 ^a	13.96±0.04 ^b
d_{c-2} (nm)	-	8.72±0.02 ^a	7.66±0.03 ^c	8.69±0.02 ^a	8.38±0.03 ^b
d_{a-2} (nm)	-	5.75±0.04 ^a	5.12±0.01 ^c	5.79±0.05 ^a	5.58±0.01 ^b

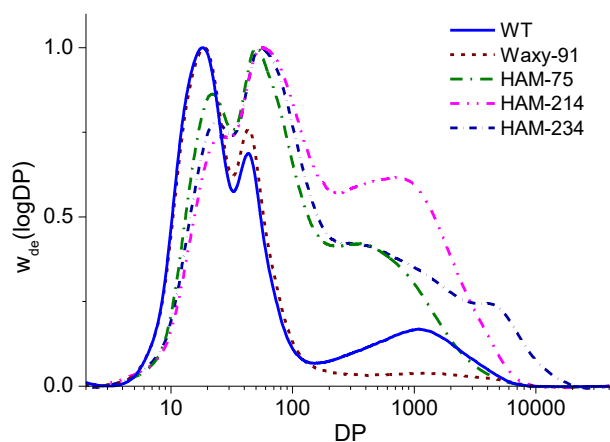
291 ^A Parameters from linear correlation function: d_1 or d_2 , the average thickness of Type I or Type II
 292 semicrystalline lamellae; d_{c-1} or d_{c-2} , the average thickness of the crystalline parts of Type I or
 293 Type II lamellae; d_{a-1} or d_{a-2} , the average thickness of the amorphous parts of Type I or Type II
 294 lamellae.

295 ^B The different inline letters within a row indicate significant difference $P < 0.05$.

296

297 **Chain Length Distributions (CLDs) of Debranched Starch Molecules.** To better understand
 298 the evolutions of starch chain features as affected by GBSSI or SBE downregulation, we detected
 299 the CLDs of debranched WT and modified sweet potato starches expressed as weight distribution

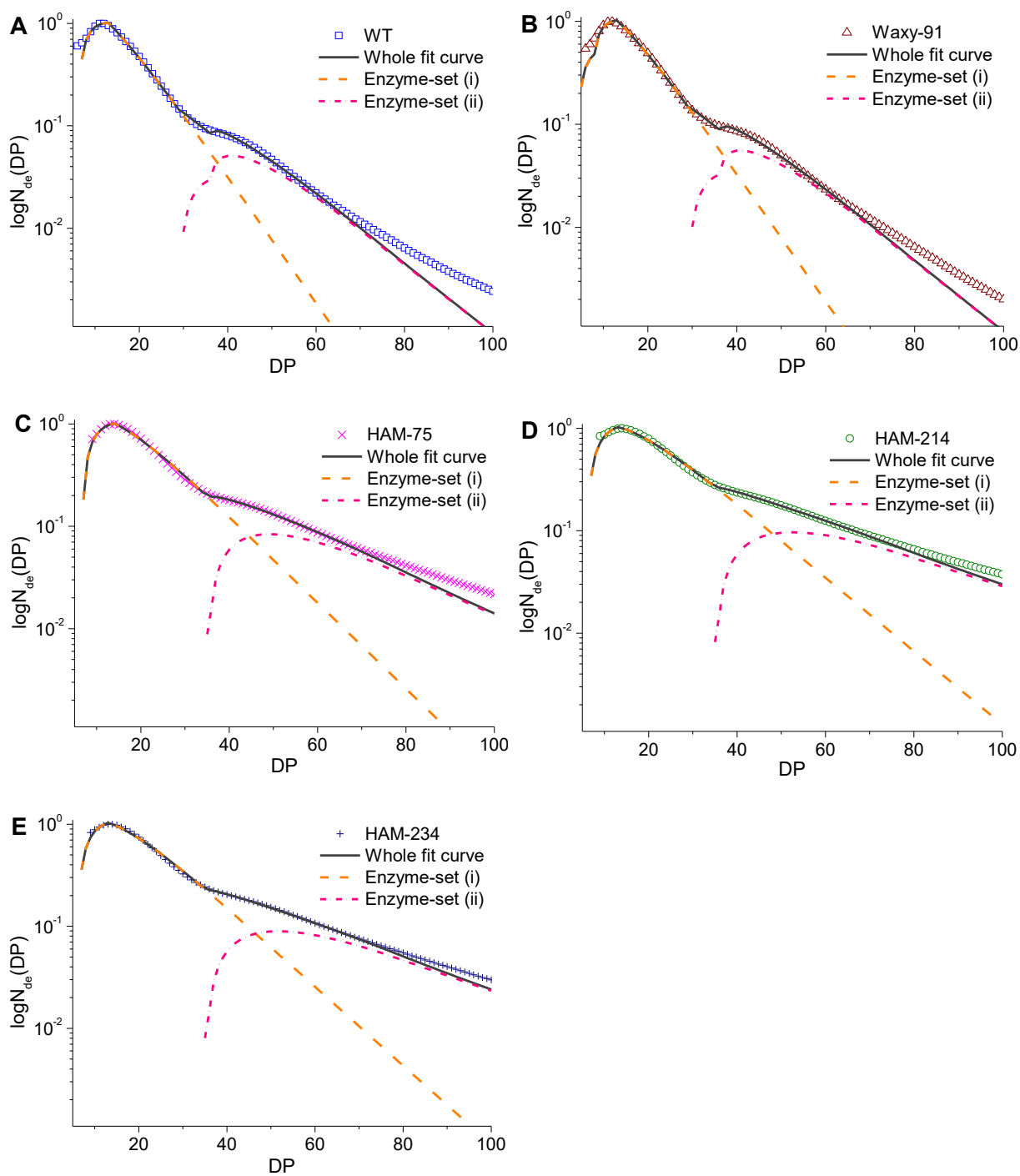
300 $w_{de}(\log DP)$ (**Fig. 4**). Despite that SEC results might suffer from inaccuracies related to band
301 broadening and the calibration between DP and elution volume⁴³, this issue is insignificant for the
302 present work for semi-quantitative purposes⁴⁴. In **Fig. 4**, the WT starch showed typical weight
303 CLDs with amylopectin chains of $DP < 100$ and amylose chains of $DP \geq 100$. There were two
304 peaks existing in the range of amylopectin chains. The first peak represents the short amylopectin
305 chains with DP up to 32, and the second peak comprises the long amylopectin chains with DP 33–
306 100. When the GBSSI activity was reduced, the resultant waxy starch displayed largely reduced
307 amylose chains (decreased apparent amylose content) but relatively increased long amylopectin
308 chains. In contrast, the SBE downregulation for high-amylose samples allowed three main kinds
309 of alteration to CLDs: (1) The first peak for short amylopectin chains centered at a higher DP but
310 still covered DP up to 32; (2) The second peak for long amylopectin chains also moved to a higher
311 DP and located in a largely-broadened range of DP 33–200; (3) The first and second peaks showed
312 a reduction and an increase in height respectively, suggesting the relatively reduced amounts of
313 short amylopectin chains or increased amounts of long amylopectin chains. These phenomena
314 became more evident when we enhanced the suppression of SBE as indicated by the increased
315 apparent amylose content. Moreover, the trend of apparent amylose content of HAM-75 < HAM-
316 234 < HAM-214 shown in the section on materials could be confirmed by the changes in the
317 relative area under the CLD curve for amylose chains.
318



319
 320 **Fig. 4** SEC weight distributions of debranched wild-type (WT) and modified (Waxy-91, HAM-
 321 75, HAM-214 and HAM-234) sweet potato starches.

322
 323 **Parameterized Biosynthetic Enzyme Activities for Starch.** The weight distributions for WT
 324 and waxy sweet potato starches were converted into the number distribution $N_{de}(DP)$ following
 325 $w_{de}(DP) = DP^2 N_{de}(DP)$,³⁶ and the number CLDs for amylopectin chains with $DP < 100$ are plotted
 326 in **Fig. 5**. A modelling method was applied to fitting the number CLDs to provide information on
 327 the relative activities of the core starch biosynthetic enzymes such as SS, SBE and DBE.³⁸ As
 328 confirmed in **Fig. 5**, the amylopectin chains were predominantly synthesized by two enzyme-sets,
 329 namely, the enzyme-set (i) fitted from $DP \leq 32$ chains (orange fit curve) and the enzyme-set (ii)
 330 fitted from DP 33 to 60–70 chains (pink fit curve).

331



335 **Fig. 5** Number chain length distributions and their fit curves of debranched wild-type (WT) (A)
336 and modified (Waxy-91, HAM-75, HAM-214 and HAM-234) (B-E) sweet potato starches. The
337 black solid line represents the whole fit curve for chains from enzyme-sets (i) and (ii); The orange

338 dash line represents the fit curve for chains from enzyme-set (i); the pink dash-dot line represents
 339 the fit curve for chains from enzyme-set (ii).

340

341 Six parameters were acquired from the fitting, including $\beta_{(i)}$ and $\beta_{(ii)}$ representing the relative
 342 activity of SBE to SS within the corresponding enzyme-set, $\gamma_{(i)}$ and $\gamma_{(ii)}$ denoting the relative
 343 activity of DBE to SS within each enzyme-set, and $h_{(i)}$ and $h_{(ii)}$ indicating the relative contribution
 344 of each enzyme-set to the whole CLDs. **Table 3** lists the fitted enzyme activity parameters. No
 345 prominent differences could be seen for the six parameters among WT and waxy sweet potato
 346 starches, reflecting that reducing GBSSI expression correlated with amylose synthesis did not
 347 significantly affect the activity ratios of SBE:SS and DBE:SS as well as the contributions of
 348 enzyme-sets to the amylopectin CLDs. However, compared to the WT starch, the values of $\beta_{(i)}$,
 349 $\beta_{(ii)}$, $\gamma_{(i)}$, and $\gamma_{(ii)}$ reduced significantly for the high-amylose starches, followed by substantially
 350 increased $h_{(ii)}$ but negligibly changed $h_{(i)}$. This indicates that reducing SBE activity caused not only
 351 an expectable reduction in the activity ratio of SBE:SS but also a decrease in the activity ratio of
 352 DBE:SS, with a relatively elevated contribution of chains from enzyme-set (ii) to the whole CLDs.
 353 Again, like for the CLD evolutions in the section on CLD results, these changes were more
 354 prominent with reduced SBE activity as indicated by the increased amylose level.

355

356 **Table 3** Parameterized biosynthetic enzyme parameters of wild-type (WT) and modified (Waxy-
 357 91, HAM-75, HAM-214 and HAM-234) sweet potato starches ^A

	WT	Waxy-91	HAM-75	HAM-214	HAM-234
$\beta_{(i)}$	0.1035±0.0016 ^{ab}	0.1047±0.0012 ^a	0.0688±0.0005 ^b	0.0598±0.0021 ^d	0.0639±0.0016 ^c
$\beta_{(ii)}$	0.0553±0.0006 ^a	0.0558±0.0003 ^a	0.0333±0.0002 ^b	0.0271±0.0003 ^d	0.0288±0.0007 ^c

$\gamma_{(i)}$	0.0599 ± 0.0004^a	0.0604 ± 0.0003^a	0.0470 ± 0.0002^b	0.0445 ± 0.0010^c	0.0463 ± 0.0007^b
$\gamma_{(ii)}$	0.0451 ± 0.0004^a	0.0450 ± 0.0005^a	0.0321 ± 0.0002^b	0.0256 ± 0.0003^d	0.0275 ± 0.0008^c
$h_{(i)}$	1.0158 ± 0.0103^{ab}	1.0239 ± 0.0066^a	1.0137 ± 0.0025^b	1.0269 ± 0.0011^a	1.0292 ± 0.0038^a
$h_{(ii)}$	0.0539 ± 0.0039^b	0.0585 ± 0.0039^b	0.0833 ± 0.0005^a	0.0906 ± 0.0082^a	0.0859 ± 0.0049^a

358 ^A $\beta_{(i)}$ or $\beta_{(ii)}$, activity ratio of SBE:SS from enzyme-set (i) or (ii); $\gamma_{(i)}$ or $\gamma_{(ii)}$, activity ratio of DBE:SS
 359 from enzyme-set (i) or (ii); $h_{(i)}$ or $h_{(ii)}$, relative contribution of enzyme-set (i) or (ii) to the whole
 360 chain length distributions.

361 ^B The different inline letters within a row indicate significant difference $P < 0.05$.

362

363 **Discussion on How GBSSI or SBE Downregulation Alters Starch Lamellae.** With the CLD

364 results and the fitted enzyme parameters, a schematic representation was proposed for the lamellar

365 structure of starch following GBSSI or SBE downregulation (**Fig. 6**). The biosynthesis of starch

366 chains and their subsequent alignment in lamellae involve the actions of different biosynthetic

367 enzymes.⁴⁵⁻⁴⁶ Particularly, the glucan chains form by transferring the glucosyl units of ADP-

368 glucose to non-reducing ends of pre-existing glucans via new α -(1,4)-linkages through soluble SSs

369 mainly for amylopectin and GBSS (GBSSI in storage tissues and GBSSII in other tissues)

370 primarily for amylose.^{45,47} SBEs create new glucan branches by catalyzing the cleavage of α -(1,4)-

371 linkages and transfer of the released reducing ends to glucose residues on the original or another

372 glucan chains via α -(1,6)-linkages.⁴⁸⁻⁴⁹ DBEs such as the isoamylases trim the improperly

373 positioned branches preventing local crystallization or side chain clustering.⁵⁰⁻⁵¹ Here, for the WT

374 starch from a regular cultivar, the enzyme-set (i) primarily but not exclusively synthesized the

375 short amylopectin chains ($DP \leq 32$) confined in single crystalline lamellae to construct the well-

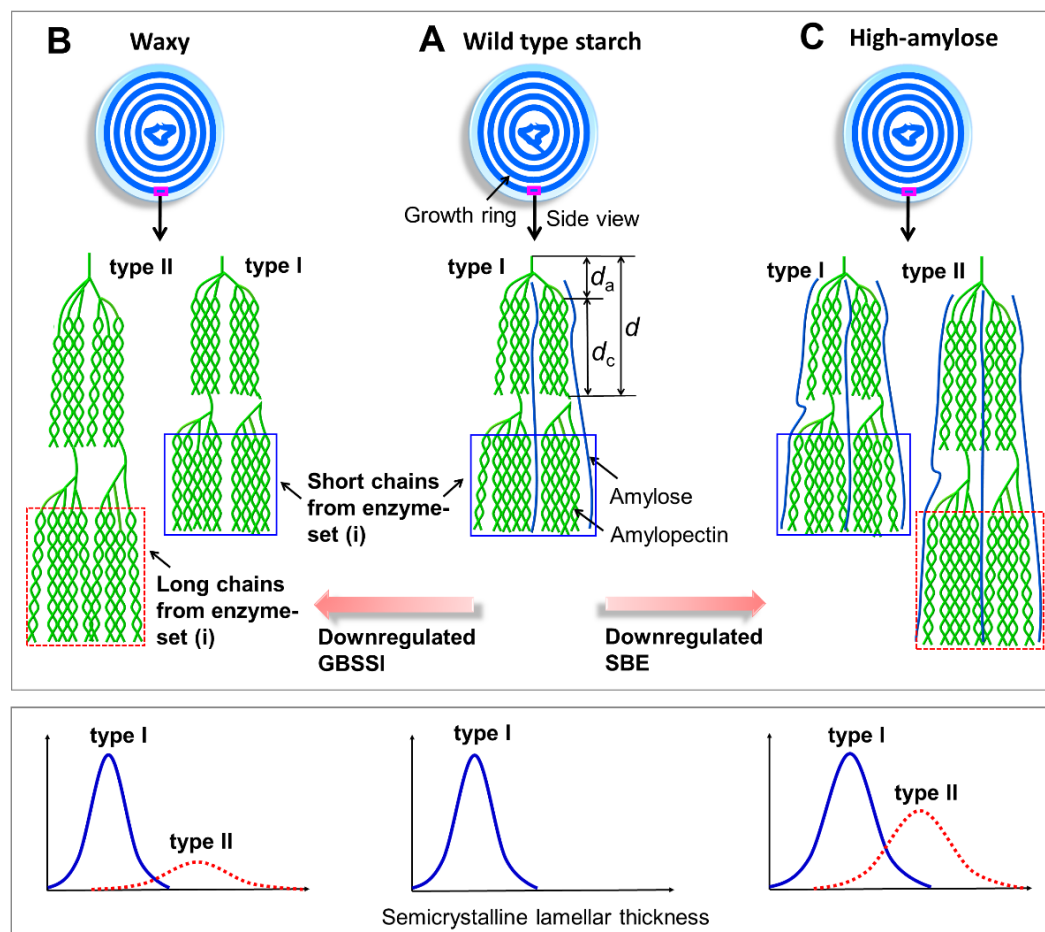
376 known lamellar structure (Type I semicrystalline lamellae in the WT starch in **Fig. 6A**), and some

377 of the long amylopectin branches ($33 \leq DP < 60-70$) protruding the single lamella space to enter

378 the contiguous amorphous lamellae (even the subsequent crystalline lamellae)³⁸. The other long

379 amylopectin chains were predominantly from the enzyme-set (ii), and protruded the single
 380 crystalline lamellae to remain in the contiguous, amorphous lamellae.^{37-38, 44}

381



382

383 **Fig. 6** Schematic representation of the lamellar structure of sweet potato starch following GBSSI
 384 or SBE downregulation. GBSSI, granule-bound starch synthase I; SBE, starch branching enzyme.

385

386 For the waxy starch, the reduced activity of GBSSI could slow the synthesis of amylose
 387 accordingly, contributing to providing relatively more glucose substrate for soluble SSI to elongate
 388 amylopectin branches. SSI elongates the shortest amylopectin chains with DP 6–7 to form DP ~9–
 389 12 chains.⁵² SSII elongates the chains from SSI to generate DP < 30 chains and the subsequent

390 products are further elongated by SSIII to create long chains (DP higher than 30).⁵³⁻⁵⁴ There are
391 two isoforms for SSII and SSIII, including SSIIa and SSIIIa in storage tissues and SSIIb and SSIIIb
392 in leave tissues.⁴⁵ Thus, it can be deduced that SSIII specifically SSIIIa in tuber had a relatively
393 stronger contribution to the synthesis of amylopectin chains, generating an increased proportion
394 of long chains with DP 33–100 (shown in **Fig. 4**). Though the formation of long amylopectin
395 chains might be also related to the reduced SBE activity,⁵⁵ the constant activity ratios of SBE:SS
396 and DBE:SS (discussed in the section on biosynthesis enzyme activities) could make this scenario
397 insignificant. Regarding the lamellar stacking, it can be proposed that part of the long amylopectin
398 chains ($DP \geq 33$) from enzyme-set (i), actually the so-called single-lamella set,³⁸ could be confined
399 to the single crystalline lamellae of Type II lamellar structure like the manner of short chains (DP
400 ≤ 32) from enzyme-set (i) to typical Type I lamellae (illustrated in **Fig. 6B**). Agreeing on this, the
401 increased lamellar thicknesses such as d_c of Type II lamellae (see the section on lamellar
402 thicknesses) confirmed the need for longer chains packed in Type II single crystalline lamellae.
403 Again, the rest of long chains from enzyme-set (i) and the long chains from enzyme-set (ii) could
404 still span more than a single-lamella range like the counterpart chains located in the WT starch.
405 Hence, this is the first work revealing that the amylopectin chains from enzyme-set (i) might be
406 classified as three subfractions rather than two subgroups reported previously³⁸, namely, the short
407 chains confined to single crystalline lamellae of Type I lamellar structure, the long chains arranged
408 to thicker single crystalline lamellae of Type II structure, and the long chains protruding single
409 crystalline lamellae.

410 For the high-amylose starches, the reduced activity ratios of SBE:SS and DBE:SS (the section
411 on biosynthesis enzyme activities) altered the chain features and thus the chain assembly in the
412 lamellar structure. Specifically, SBE has two types, involving SBEI and SBEII preferentially

413 transferring the glucan chains of different lengths. SBEI is apt to branch long chains such as
414 amylose and transfer longer branches; SBEII tends to branch highly-branched amylopectin and
415 transfer short branches.⁴⁹ The reduced SBEII expression, with the SSs still elongating amylopectin
416 chains, certainly hindered the generation of short amylopectin chains (reflected by the shift of the
417 short chain peak to higher *DP* values in **Fig. 4** in the section on CLD results) but significantly
418 enhanced the formation of long amylopectin chains (confirmed by the stronger peak for long
419 chains in **Fig. 4**). The lowered activity of SBEI and the steady action of GBSS to elongate amylose
420 chains could allow the synthesis of increased amylose chains probably with higher *DP* values
421 (shown in **Fig. 4**). In addition, the lowered SBE activity with normal SSs including GBSS reduced
422 the possibility for the generation of improperly positioned chains, weakening the need of DBEs to
423 trim these chains (see reduced DBE:SS activity ratio in the section on biosynthesis enzyme
424 activities). Analogous to the lamellae in the waxy starch, Type I lamellae were mainly constructed
425 by $DP \leq 32$ short chains from the single-lamella enzyme-set (i); the right-shifted peak of these
426 short chains (suggesting an increased average chain length) resulted in the emergence of thickened
427 crystalline lamellae (an increased d_c) constructing the semicrystalline lamellae with a larger d .
428 Type II crystalline lamellae contained part of long amylopectin chains with *DP* above 33 to form
429 the related lamellar structure with an increase average thickness (**Fig. 6C**). Again, the enhancement
430 of SBE downregulation could enhance the evolutions in chain features and thus in the lamellar
431 structural parameters.

432 To conclude, the downregulated GBSSI or SBE activity could give rise to the formation of
433 additional semicrystalline lamellae (named Type II) in sweet potato starch, other than the typical
434 lamellae (Type I) found previously. A fitting approach based on two Gaussian plus Lorentz peak
435 functions with a power-law function was established to successfully resolve the net lamellar peak

436 and its two subpeaks related to Type I and Type II lamellar structures respectively from the whole
437 SAXS pattern; then, the fine features of the two kinds of amorphous-crystalline lamellae were
438 disclosed with the linear correlation function. Relative to Type I lamellae, Type II lamellae showed
439 increases in the average thickness (d) and the thickness distribution width ($FWHM$), followed by
440 simultaneously thickened amorphous (d_a) and crystalline (d_c) parts. These lamellar structural
441 features could be further regulated by simply controlling the enzyme type (*e.g.*, GBSSI and SBE)
442 for activity downregulation and the activity downregulation degree for a specific enzyme such as
443 SBE.

444 Then, the chain length distributions in sweet potato starches and the relative activities of
445 biosynthetic enzymes were analyzed to help understand how the reduced GBSSI or SBE activity
446 influences the starch lamellar structure. Note that mainly two starch biosynthetic enzyme-sets,
447 namely, enzyme-set (i) and enzyme-set (ii), were confirmed to synthesize the glucan chains of
448 amylopectin. Along with the actions of other biosynthetic enzymes, the decreased GBSSI or SBE
449 activity tended to relatively increase the amount of amylopectin long chains with a degree of
450 polymerization (DP) ≥ 33 . Part of these long chains from the single-lamella enzyme-set (i) could
451 be confined to the single crystalline lamella space of Type II lamellar structure, whereas the short
452 chains of $DP \leq 32$ could be aligned within the crystalline parts of Type I lamellae, with the rest
453 long chains from enzyme-set (i) and the long chains from enzyme-set (ii) located in more than a
454 single lamella. Hence, this work enables an in-depth understanding of the new lamellar structural
455 features in sweet potato starch as induced by GBSSI or SBE downregulation, which is valuable
456 for the rational production of similar starch resources with regulated structure and thus
457 performance for different food products.

458 ASSOCIATED CONTENT

459 **Supporting Information (SI)** is available free of charge on the ACS Publications website at
460 DOI: xxx. See SI for supplementary Tables and Figure.

461 AUTHOR INFORMATION

462 **Corresponding Author**

463 * Peng Zhang. Email: zhangpeng@sibs.ac.cn

464 † Fengwei Xie. Email: f.xie@uq.edu.au, fwhsieh@gmail.com

465 **Author Contributions**

466 The manuscript was written through contributions of all authors. All authors have given approval
467 to the final version of the manuscript.

468 **Notes**

469 The authors declare no competing financial interest.

470 ACKNOWLEDGMENT

471 The authors would like to acknowledge the National Natural Science Foundation of China (NSFC)
472 (Project Nos. 31701637 and 31801582), the Fundamental Research Funds for the Central
473 Universities (Project No. 2662016QD008), the Chinese Academy of Sciences (Project No.
474 XDPB04), and the Project funded by China Postdoctoral Science Foundation (Project No.
475 2018M642865). B. Zhang thanks the Young Elite Scientists Sponsorship Program by China
476 Association for Science and Technology, the Chutian Sholars Program of Hubei Province, and the
477 Shishan Sholars Program of Huazhong Agricultural University. F. Xie acknowledges the support
478 of the European Union's Marie Skłodowska-Curie Actions (MSCA) and the Institute of Advanced

479 Study (IAS), University of Warwick for the Warwick Interdisciplinary Research Leadership
480 Programme (WIRL-COFUND). The authors also thank Dr. Cheng Li, Dr. Enpeng Li and Mr.
481 Shiqing Zhou from Prof. Robert G. Gilbert's lab at Yangzhou University for their assistance on
482 SEC analysis.

483 ABBREVIATIONS

484 GBSSI, Granule-bound starch synthase I; SBE, starch branching enzyme; DP, degree of
485 polymerization; AGPase, ADP-glucose pyrophosphorylase; SSs, starch synthases; SBEs, starch
486 branching enzymes; DBEs, starch debranching enzymes; WT, wild-type; SAXS, small-angle X-
487 ray scattering; CLDs, chain length distributions; FWHM, peak full width at half-maximum.

488 REFERENCES

- 489 1. Lee, Y.; Choi, M.-S.; Lee, G.; Jang, S.; Yoon, M.-R.; Kim, B.; Piao, R.; Woo, M.-O.; Chin, J. H.;
490 Koh, H.-J., Sugary Endosperm is Modulated by Starch Branching Enzyme Iia in Rice (*Oryza sativa* L.).
491 *Rice* **2017**, *10* (1), 33.
- 492 2. Wang, Y.; Li, Y.; Zhang, H.; Zhai, H.; Liu, Q.; He, S., A soluble starch synthase I gene, IbSSI,
493 alters the content, composition, granule size and structure of starch in transgenic sweet potato. *Sci. Rep.*
494 **2017**, *7* (1), 2315-2315.
- 495 3. Zobel, H. F., Molecules to Granules: A Comprehensive Starch Review. *Starch - Stärke* **1988**, *40*
496 (2), 44-50.
- 497 4. French, D., Fine Structure of Starch and its Relationship to the Organization of Starch Granules.
498 *Journal of the Japanese Society of Starch Science* **1972**, *19* (1), 8-25.
- 499 5. Tester, R. F.; Karkalas, J.; Qi, X., Starch—composition, fine structure and architecture. *J. Cereal*
500 *Sci.* **2004**, *39* (2), 151-165.
- 501 6. Donald, A. M.; Waigh, T. A.; Jenkins, P. J.; Gidley, M. J.; Debet, M.; Smith, A., Internal structure
502 of starch granules revealed by scattering studies. In *Starch: Structure and Functionality*, Frazier, P. J.;

- 503 Donald, A. M.; Richmond, P., Eds. The Royal Society of Chemistry: Cambridge, 1997; pp 172-179.
- 504 7. Zhou, W.; Yang, J.; Hong, Y.; Liu, G.; Zheng, J.; Gu, Z.; Zhang, P., Impact of amylose content on
505 starch physicochemical properties in transgenic sweet potato. *Carbohydr. Polym.* **2015**, *122*, 417-427.
- 506 8. Jobling, S., Improving starch for food and industrial applications. *Curr. Opin. Plant Biol.* **2004**, *7*
507 (2), 210-218.
- 508 9. Qiao, D.; Yu, L.; Liu, H.; Zou, W.; Xie, F.; Simon, G.; Petinakis, E.; Shen, Z.; Chen, L., Insights
509 into the hierarchical structure and digestion rate of alkali-modulated starches with different amylose
510 contents. *Carbohydr. Polym.* **2016**, *144*, 271-281.
- 511 10. Blazek, J.; Gilbert, E. P., Effect of Enzymatic Hydrolysis on Native Starch Granule Structure.
512 *Biomacromolecules* **2010**, *11* (12), 3275-3289.
- 513 11. Liu, H. S.; Xie, F. W.; Yu, L.; Chen, L.; Li, L., Thermal processing of starch-based polymers. *Prog.*
514 *Polym. Sci.* **2009**, *34* (12), 1348-1368.
- 515 12. Xie, F.; Halley, P. J.; Avérous, L., Rheology to understand and optimize processibility, structures
516 and properties of starch polymeric materials. *Prog. Polym. Sci.* **2012**, *37* (4), 595-623.
- 517 13. Cameron, R. E.; Donald, A. M., A Small-Angle X-Ray-Scattering Study of the Absorption of Water
518 into the Starch Granule. *Carbohydr. Res.* **1993**, *244* (2), 225-236.
- 519 14. Cameron, R. E.; Donald, A. M., A Small-Angle X-Ray-Scattering Study of Starch Gelatinization
520 in Excess and Limiting Water. *Journal of Polymer Science Part B-Polymer Physics* **1993**, *31* (9), 1197-
521 1203.
- 522 15. Daniels, D. R.; Donald, A. M., Soft material characterization of the lamellar properties of starch:
523 Smectic side-chain liquid-crystalline polymeric approach. *Macromolecules* **2004**, *37* (4), 1312-1318.
- 524 16. Zhang, B.; Chen, L.; Li, X.; Li, L.; Zhang, H., Understanding the multi-scale structure and
525 functional properties of starch modulated by glow-plasma: A structure-functionality relationship. *Food*
526 *Hydrocolloid* **2015**, *50*, 228-236.
- 527 17. Qiao, D.; Tu, W.; Zhang, B.; Wang, R.; Li, N.; Nishinari, K.; Riffat, S.; Jiang, F., Understanding
528 the multi-scale structure and digestion rate of water chestnut starch. *Food Hydrocolloid* **2019**, *91*, 311-318.

- 529 18. Hernández-Hernández, E.; Ávila-Orta, C. A.; Hsiao, B. S.; Castro-Rosas, J.; Gallegos-Infante, J.
530 A.; Morales-Castro, J.; Araceli Ochoa-Martínez, L.; Gómez-Aldapa, C. A., Synchrotron X-ray scattering
531 analysis of the interaction between corn starch and an exogenous lipid during hydrothermal treatment. *J.*
532 *Cereal Sci.* **2011**, *54* (1), 69-75.
- 533 19. Gomand, S. V.; Lamberts, L.; Gommès, C. J.; Visser, R. G.; Delcour, J. A.; Goderis, B., Molecular
534 and morphological aspects of annealing-induced stabilization of starch crystallites. *Biomacromolecules*
535 **2012**, *13* (5), 1361-70.
- 536 20. Bie, P.; Li, X.; Xie, F.; Chen, L.; Zhang, B.; Li, L., Supramolecular structure and thermal behavior
537 of cassava starch treated by oxygen and helium glow-plasmas. *Innov. Food Sci. Emerg.* **2016**, *34*, 336-343.
- 538 21. Blazek, J.; Gilbert, E. P., Application of small-angle X-ray and neutron scattering techniques to the
539 characterisation of starch structure: A review. *Carbohydr. Polym.* **2011**, *85* (2), 281-293.
- 540 22. Koroteeva, D. A.; Kiseleva, V. I.; Krivandin, A. V.; Shatalova, O. V.; Blaszcak, W.; Bertoft, E.;
541 Piyachomkwan, K.; Yuryev, V. P., Structural and thermodynamic properties of rice starches with different
542 genetic background Part 2. Defectiveness of different supramolecular structures in starch granules. *Int J*
543 *Biol Macromol* **2007**, *41* (5), 534-47.
- 544 23. Koroteeva, D. A.; Kiseleva, V. I.; Sriroth, K.; Piyachomkwan, K.; Bertoft, E.; Yuryev, P. V.;
545 Yuryev, V. P., Structural and thermodynamic properties of rice starches with different genetic background:
546 Part 1. Differentiation of amylopectin and amylose defects. *Int J Biol Macromol* **2007**, *41* (4), 391-403.
- 547 24. Yang, J.; Bi, H.-P.; Fan, W.-J.; Zhang, M.; Wang, H.-X.; Zhang, P., Efficient embryogenic
548 suspension culturing and rapid transformation of a range of elite genotypes of sweet potato (*Ipomoea batatas*
549 [L.] Lam.). *Plant Sci.* **2011**, *181* (6), 701-711.
- 550 25. Zhao, S.; Dufour, D.; Sánchez, T.; Ceballos, H.; Zhang, P., Development of waxy cassava with
551 different Biological and physico-chemical characteristics of starches for industrial applications. *Biotechnol.*
552 *Bioeng.* **2011**, *108* (8), 1925-1935.
- 553 26. Tan, I.; Flanagan, B. M.; Halley, P. J.; Whittaker, A. K.; Gidley, M. J., A method for estimating
554 the nature and relative proportions of amorphous, single, and double-helical components in starch granules

- 555 by C-13 CP/MAS NMR. *Biomacromolecules* **2007**, *8* (3), 885-891.
- 556 27. Zhang, B.; Bai, B.; Pan, Y.; Li, X. M.; Cheng, J. S.; Chen, H. Q., Effects of pectin with different
557 molecular weight on gelatinization behavior, textural properties, retrogradation and in vitro digestibility of
558 corn starch. *Food Chem.* **2018**, *264*, 58-63.
- 559 28. Waigh, T. A.; Perry, P.; Riekel, C.; Gidley, M. J.; Donald, A. M., Chiral side-chain liquid-
560 crystalline polymeric properties of starch. *Macromolecules* **1998**, *31* (22), 7980-7984.
- 561 29. Waigh, T. A.; Kato, K. L.; Donald, A. M.; Gidley, M. J.; Clarke, C. J.; Riekel, C., Side-chain liquid-
562 crystalline model for starch. *Starch/Stärke* **2000**, *52* (12), 450-460.
- 563 30. Suzuki, T.; Chiba, A.; Yano, T., Interpretation of small angle X-ray scattering from starch on the
564 basis of fractals. *Carbohydr. Polym.* **1997**, *34* (4), 357-363.
- 565 31. Goderis, B.; Reynaers, H.; Koch, M. H. J.; Mathot, V. B. F., Use of SAXS and linear correlation
566 functions for the determination of the crystallinity and morphology of semi-crystalline polymers.
567 Application to linear polyethylene. *Journal of Polymer Science Part B-Polymer Physics* **1999**, *37* (14),
568 1715-1738.
- 569 32. Wang, C.; Liao, W. P.; Cheng, Y. W., Strong diffuse scattering and lamellar morphologies of
570 syndiotactic polystyrene: Polymorphic effects. *Journal of Polymer Science Part B-Polymer Physics* **2003**,
571 *41* (20), 2457-2469.
- 572 33. Qiao, D.; Xie, F.; Zhang, B.; Zou, W.; Zhao, S.; Niu, M.; Lv, R.; Cheng, Q.; Jiang, F.; Zhu, J., A
573 further understanding of the multi-scale supramolecular structure and digestion rate of waxy starch. *Food*
574 *Hydrocolloids* **2017**, *65*, 24-34.
- 575 34. Shi, L. F.; Fu, X.; Tan, C. P.; Huang, Q.; Zhang, B., Encapsulation of Ethylene Gas into Granular
576 Cold-Water-Soluble Starch: Structure and Release Kinetics. *J. Agric. Food Chem.* **2017**, *65* (10), 2189-
577 2197.
- 578 35. Hasjim, J.; Lavau, G. C.; Gidley, M. J.; Gilbert, R. G., In Vivo and In Vitro Starch Digestion: Are
579 Current in Vitro Techniques Adequate? *Biomacromolecules* **2010**, *11* (12), 3600-3608.
- 580 36. Liu, W.-C.; Halley, P. J.; Gilbert, R. G., Mechanism of Degradation of Starch, a Highly Branched

- 581 Polymer, during Extrusion. *Macromolecules* **2010**, *43* (6), 2855-2864.
- 582 37. Wu, A. C.; Gilbert, R. G., Molecular Weight Distributions of Starch Branches Reveal Genetic
583 Constraints on Biosynthesis. *Biomacromolecules* **2010**, *11* (12), 3539-3547.
- 584 38. Wu, A. C.; Morell, M. K.; Gilbert, R. G., A Parameterized Model of Amylopectin Synthesis
585 Provides Key Insights into the Synthesis of Granular Starch. *PLoS ONE* **2013**, *8* (6).
- 586 39. Zhang, B.; Xie, F.; Shamshina, J. L.; Rogers, R. D.; McNally, T.; Halley, P. J.; Truss, R. W.; Chen,
587 L.; Zhao, S., Dissolution of Starch with Aqueous Ionic Liquid under Ambient Conditions. *ACS Sustainable*
588 *Chemistry & Engineering* **2017**, *5* (5), 3737-3741.
- 589 40. Shrestha, A. K.; Blazek, J.; Flanagan, B. M.; Dhital, S.; Larroque, O.; Morell, M. K.; Gilbert, E. P.;
590 Gidley, M. J., Molecular, mesoscopic and microscopic structure evolution during amylase digestion of
591 maize starch granules. *Carbohydr. Polym.* **2012**, *90* (1), 23-33.
- 592 41. Zhang, B.; Xie, F.; Wang, D. K.; Zhao, S.; Niu, M.; Qiao, D.; Xiong, S.; Jiang, F.; Zhu, J.; Yu, L.,
593 An improved approach for evaluating the semicrystalline lamellae of starch granules by synchrotron SAXS.
594 *Carbohydr. Polym.* **2017**, *158*, 29-36.
- 595 42. Cardoso, M. B.; Westfahl, H., On the lamellar width distributions of starch. *Carbohydr. Polym.*
596 **2010**, *81* (1), 21-28.
- 597 43. Cave, R. A.; Seabrook, S. A.; Gidley, M. J.; Gilbert, R. G., Characterization of Starch by Size-
598 Exclusion Chromatography: The Limitations Imposed by Shear Scission. *Biomacromolecules* **2009**, *10* (8),
599 2245-2253.
- 600 44. Wang, K.; Hasjim, J.; Wu, A. C.; Henry, R. J.; Gilbert, R. G., Variation in Amylose Fine Structure
601 of Starches from Different Botanical Sources. *J. Agric. Food Chem.* **2014**, *62* (19), 4443-4453.
- 602 45. Tetlow, I. J., Starch biosynthesis in developing seeds. *Seed Science Research* **2011**, *21* (1), 5-32.
- 603 46. Castro, J. V.; Dumas, C.; Chiou, H.; Fitzgerald, M. A.; Gilbert, R. G., Mechanistic information
604 from analysis of molecular weight distributions of starch. *Biomacromolecules* **2005**, *6* (4), 2248-2259.
- 605 47. Ball, S. G.; Morell, M. K., From bacterial glycogen to starch: Understanding the biogenesis of the
606 plant starch granule. *Annu. Rev. Plant Biol.* **2003**, *54*, 207-233.

- 607 48. Rahman, S.; Regina, A.; Li, Z. Y.; Mukai, Y.; Yamamoto, M.; Kosar-Hashemi, B.; Abrahams, S.;
608 Morell, M. K., Comparison of starch-branching enzyme genes reveals evolutionary relationships among
609 isoforms. Characterization of a gene for starch-branching enzyme IIa from the wheat D genome donor
610 *Aegilops tauschii*. *Plant Physiol.* **2001**, *125* (3), 1314-1324.
- 611 49. Nakamura, Y.; Utsumi, Y.; Sawada, T.; Aihara, S.; Utsumi, C.; Yoshida, M.; Kitamura, S.,
612 Characterization of the Reactions of Starch Branching Enzymes from Rice Endosperm. *Plant Cell Physiol*
613 **2010**, *51* (5), 776-794.
- 614 50. Delatte, T.; Trevisan, M.; Parker, M. L.; Zeeman, S. C., Arabidopsis mutants Atisa1 and Atisa2
615 have identical phenotypes and lack the same multimeric isoamylase, which influences the branch point
616 distribution of amylopectin during starch synthesis. *Plant J.* **2005**, *41* (6), 815-830.
- 617 51. Wattebled, F.; Planchot, V.; Dong, Y.; Szydlowski, N.; Pontoire, B.; Devin, A.; Ball, S.; D'Hulst,
618 C., Further Evidence for the Mandatory Nature of Polysaccharide Debranching for the Aggregation of
619 Semicrystalline Starch and for Overlapping Functions of Debranching Enzymes in Arabidopsis Leaves.
620 *Plant Physiol.* **2008**, *148* (3), 1309-1323.
- 621 52. Fujita, N.; Yoshida, M.; Asakura, N.; Ohdan, T.; Miyao, A.; Hirochika, H.; Nakamura, Y., Function
622 and characterization of starch synthase I using mutants in rice. *Plant Physiol.* **2006**, *140* (3), 1070-1084.
- 623 53. Umemoto, T.; Yano, M.; Satoh, H.; Shomura, A.; Nakamura, Y., Mapping of a gene responsible
624 for the difference in amylopectin structure between japonica-type and indica-type rice varieties. *Theor Appl*
625 *Genet* **2002**, *104* (1), 1-8.
- 626 54. Fujita, N.; Yoshida, M.; Kondo, T.; Saito, K.; Utsumi, Y.; Tokunaga, T.; Nishi, A.; Satoh, H.; Park,
627 J.-H.; Jane, J.-L.; Miyao, A.; Hirochika, H.; Nakamura, Y., Characterization of SSIIIa-Deficient mutants of
628 rice: The function of SSIIIa and pleiotropic effects by SSIIIa deficiency in the rice endosperm. *Plant Physiol.*
629 **2007**, *144* (4), 2009-2023.
- 630 55. Wang, K.; Wambugu, P. W.; Zhang, B.; Wu, A. C.; Henry, R. J.; Gilbert, R. G., The biosynthesis,
631 structure and gelatinization properties of starches from wild and cultivated African rice species (*Oryza*
632 *barthii* and *Oryza glaberrima*). *Carbohydr. Polym.* **2015**, *129*, 92-100.
- 633

- Table of Contents -

Changes in Nanoscale Chain Assembly in Sweet Potato Starch Lamellae by Downregulation of Biosynthesis Enzymes

Binjia Zhang^a, Wenzhi Zhou^b, Dongling Qiao^c, Peng Zhang^{*,b}, Siming Zhao^a, Liang Zhang^d,
Fengwei Xie^{†,e,f}

